# Coulomb entangler and entanglement-testing network for waveguide qubits

Linda E. Reichl and Michael G. Snyder
*Center for Studies in Statistical Mechanics and Complex Systems, The University of Texas at Austin, Austin, Texas 78712, USA*
(Received 6 May 2005; published 26 September 2005)

We present a small network for the testing of the entanglement of two ballistic electron waveguide qubits. The network produces different output conditional on the presence or absence of entanglement. The structure of the network allows for the determination of successful entanglement operations through the measurement of the output of a single qubit. We also present a simple model of a dynamic Coulomb-like interaction and use it to describe some characteristics of a proposed scheme for the entanglement of qubits in ballistic electron waveguides.

DOI: 10.1103/PhysRevA.72.032330 PACS number(s): 03.67.Mn, 03.65.Ud, 73.23.Ad

## I. INTRODUCTION

A simple quantum computer consists of an array of qubits and a series of gates formed by single-qubit and two-qubit unitary transformations. A single-qubit gate rotates the state of the qubit. The two-qubit gate creates an entangled pair of qubits. Any proposed system for quantum computation must provide a mechanism for pairwise entanglement of qubits.

The possibility of performing quantum computation in ballistic electron waveguides was first proposed by Ioniciou *et al.* [1]. In their approach, a single-electron wave packet and two parallel waveguides are used to form a "flying qubit," with one waveguide designated as the $|0\rangle$ state and the other as the $|1\rangle$ state. Subsequent work by Akguc *et al.* [2] and Snyder and Reichl [3] focused on the computation of *stationary states of networks* (rather than use the time evolution of wave packets) of such qubits. They showed that it is possible to obtain stationary-state solutions to the Schrödinger equation for fairly complex quantum networks of qubits and quqits.

One proposed mechanism for the entanglement of waveguide-based qubits is the Coulomb interaction between electrons in different qubits. For example, a small segment of the waveguides in two qubits (which we call qubit *A* and qubit *B*) which represent the $|1\rangle$ state could be brought close to one another or could be separated by a dielectric that allows interaction between electrons in the $|1\rangle$ waveguides. This must be done in such a manner that electrons cannot tunnel between the qubits (see Fig. 1). If electrons in the $|1\rangle$ waveguides pass the interaction region at the same time, they can interact and create a phase change in the network state $|1, 1\rangle$ with no change in the remaining states $|1, 0\rangle$, $|0, 1\rangle$, and $|0, 0\rangle$. This is sufficient to entangle the network. In Akguc *et al.* [2] a simple static model of this entanglement mechanism showed that a phase change of $e^{i\pi}$ could be achieved for the state $|1, 1\rangle$. In subsequent sections, we analyze a dynamic model of the electron scattering process in the interaction region which confirms this prediction. We also analyze a simple two-qubit network which could allow a test for the efficiency of this entanglement mechanism.

The waveguide structures we consider can be formed at the interface of a $GaAs/Al_xGa_{1-x}As$ semiconductor heterostructure. At temperatures, $T \sim 0.1-2.0$ K, an electron travels ballistically with a phase coherence length of the order of $L_\phi \sim 30-40$ $\mu$m [4]. The gate structures themselves have been shown to be anywhere from 0.17 to 0.4 $\mu$m in length [2,5]. The small network presented here contains few enough gates to be realizable with the coherence length presently achievable in semiconductor heterostructures.

In Sec. II, we will present an electron waveguide network consisting of two qubits and a series of single-qubit and two-qubit gates which can be used to test for entanglement. We first construct the network with ideal single-qubit transformations and ideal entangling two-qubit transformations. We also construct the network with nonideal entanglement gates and compare the outputs to the idealized case. We will see that the output of the nonideal network could be used to determine whether or not the entanglement gates behave as expected. Then, in Sec. III, we present a simple model of an electron scattering process that can achieve entanglement of a pair of qubits. A classical description of the dynamics is first discussed, and then a steady-state quantum scattering analysis of the same model is used to describe the behavior of the mutual phase acquired by the entangled electron current in the pair of waveguides. In Sec. IV, we make some concluding remarks.

## II. ENTANGLEMENT TESTING NETWORK

In this section, we describe a simple quantum network that can test the effectiveness of an entanglement gate. The network is shown in Fig. 2. It consists of a sequence of

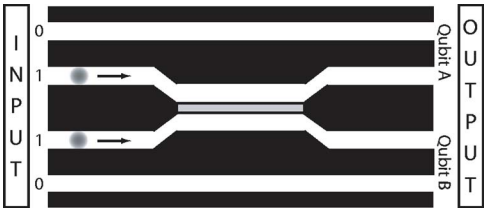


FIG. 1. (Color online) Each qubit is a pair of waveguides. The spatial location of the electron in the waveguides determines the state of the qubit. Here both qubits are in state $|1\rangle$. The waveguides representing state $|1\rangle$ are brought near each other to facilitate the Coulomb interaction of the electrons, effecting a two-qubit unitary transformation.

 

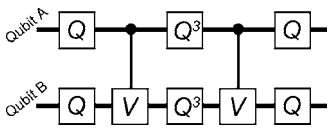


FIG. 2. A schematic of the entanglement testing network. Boxes represent individual transformations. $Q$ and $Q^3$ are single-qubit transformations. $V$ is a two-qubit transformation.

single-qubit $\sqrt{\text{NOT}}$ gates $\hat{Q}$ and two-qubit entanglement gates $\hat{V}$. (In Akguc *et al.* [2], it was shown that a single-qubit $\sqrt{\text{NOT}}$ gate could be constructed in electron waveguides by using a properly constructed cavity which connects the two waveguide leads of the qubit.) Electrons are injected into the network from the left in a state $|\Phi_L\rangle = c_1|0,0\rangle + c_2|0,1\rangle + c_3|1,0\rangle + c_4|1,1\rangle$. This state is then acted on by a sequence of gates

$$\hat{N} = \hat{Q}_B \cdot \hat{Q}_A \cdot \hat{V}_{AB} \cdot \hat{Q}_B^3 \cdot \hat{Q}_A^3 \cdot \hat{V}_{AB} \cdot \hat{Q}_B \cdot \hat{Q}_A, \tag{1}$$

where

$$Q_A = \frac{1}{2}\begin{pmatrix} 1+i & 0 & 1-i & 0 \\ 0 & 1+i & 0 & 1-i \\ 1-i & 0 & 1+i & 0 \\ 0 & 1-i & 0 & 1+i \end{pmatrix}, \tag{2}$$

$$Q_B = \frac{1}{2}\begin{pmatrix} 1+i & 1-i & 0 & 0 \\ 1-i & 1+i & 0 & 0 \\ 0 & 0 & 1+i & 1-i \\ 0 & 0 & 1-i & 1+i \end{pmatrix}, \tag{3}$$

and

$$V = \begin{pmatrix} 1 & 0 & 0 & 0 \\ 0 & e^{i\phi_1} & 0 & 0 \\ 0 & 0 & e^{i\phi_2} & 0 \\ 0 & 0 & 0 & e^{i\theta} \end{pmatrix}. \tag{4}$$

All three matrices act on the state vector $\Phi_L = (c_1, c_2, c_3, c_4)^T$, where $T$ denotes transpose. We write the two-qubit entanglement matrix in terms of phases $\phi_1$, $\phi_2$, and $\theta$, so we can describe some general features of this matrix.

When $\hat{N}$ acts on the input state $|\Phi_L\rangle$, we obtain an output state $|\Phi_R\rangle = \hat{N}|\Phi_L\rangle$, which gives the distribution of electrons exiting the quantum network on the right. For example, if $\phi_1 = \phi_2 = 0$ and $\theta = \pi$, an input state $|\Phi_L\rangle = |1,1\rangle$ on the left leads to an output state $|\Phi_R\rangle = e^{i3\pi/2}|0,1\rangle$ on the right. In this example a series of single-qubit operations and two entanglement operations produces an unentangled output state. Although the output state is unentangled, the particular form of the output state will depend upon a successful entanglement of the qubits in the middle of the computation.

We can indirectly test if the gate $\hat{V}$ is successful in entangling the two qubits by means of the network outlined above. A specific realization of the gate $\hat{V}$ is defined by the choice of the parameters $\phi_1$, $\phi_2$, and $\theta$. Through these parameters we define two types of the gate $\hat{V}$, one which entangles the qubits and one which does not. As the parameters are varied the output of the network is found for both types of $\hat{V}$ gate. We find that the entangling gate and the nonentangling gate give very different outputs in both the two-qubit and one-qubit bases, allowing for the determination of successful entangling operations in the network through the measurement of the output of only one of the qubits.

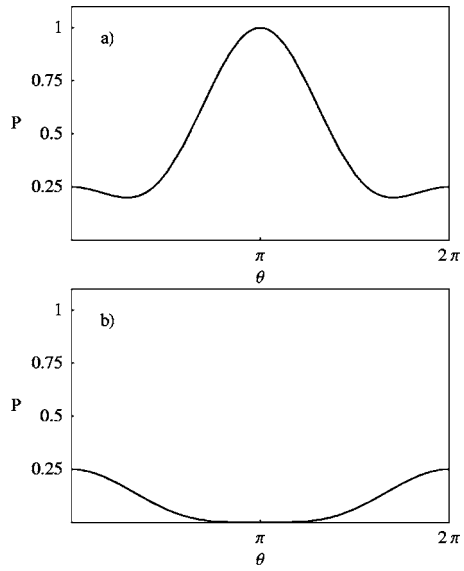


FIG. 3. A plot of the probability of finding the output state $|1, 0\rangle$ as a function of the phase angle $\theta$ for both the entangled and unentangled cases. (a) Entangled network with $\phi_1 = \phi_2 = 0$. (b) Unentangled network with $\phi_1 = \phi_2 = \theta/2$. When $\theta$ is near $\pi$ the entangled and unentangled situations are most easily distinguished.

A perfect entanglement gate $\hat{V}$ changes the phase only of the two-qubit state $|1, 1\rangle$ and is represented by $\hat{V}$ where $\phi_1 = \phi_2 = 0$ and $\theta = \pi$. A two-qubit gate that does not entangle the qubits changes the phase of the single-qubit states $|1_A\rangle$ and $|1_B\rangle$ so that the two qubits remain separable. Such a gate is represented by the matrix $\hat{V}$ where $\phi_1 + \phi_2 = \theta$. Due to the spatial symmetry of the quantum network, we can choose $\phi_1 = \phi_2 = \theta/2$ to represent a nonentangling two-qubit gate. Therefore, if we begin with an input state $|\Phi_L\rangle = |1,1\rangle$ and act on it with a network $\hat{N}$ containing the perfect entangling gate $\hat{V}$, where $\theta = \pi$ and $\phi_1 = \phi_2 = 0$, we find, as above, $\hat{N}|1,1\rangle = e^{i3\pi/2}|0,1\rangle$. A network containing the nonentangling gate where $\phi_1 = \phi_2 = \pi/2$ and $\theta = \pi$ gives $\hat{N}|1,1\rangle = e^{i3\pi/2}|1,0\rangle$, which is easily distinguishable from the case when entanglement is present. In Fig. 3, we plot the probability $P = |\langle\Phi_R|0,1\rangle|^2$ of finding the ideal output $|\Phi_L\rangle = |0,1\rangle$ as a function of $\theta$ for both the entangled case and the unentangled case. We find that the respective outputs are most different when $\theta = \pi$ and equal when no phase change occurs.

We can find the amount of probability exiting an individual waveguide in a given network by

$$\text{Prob}_A(|1\rangle) = \langle\Phi_R|(|1\rangle\langle 1|)|\Phi_R\rangle. \tag{5}$$

The probability of finding electrons in the $|0\rangle$ and $|1\rangle$ states of qubit $A$ for both the entangled network and the unentangled

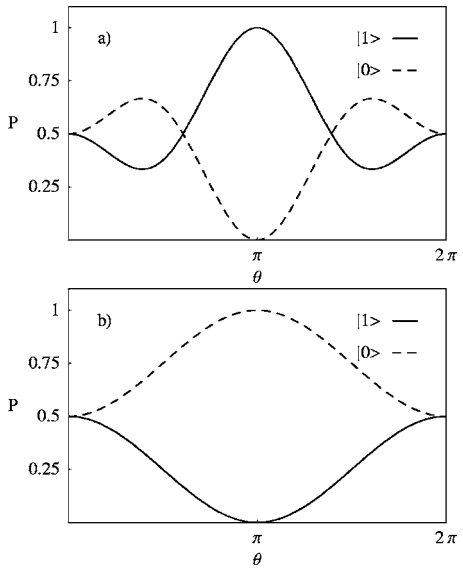


FIG. 4. The output probability for each state of qubit $A$. (a) Entangled network with $\phi_1=\phi_2=0$. (b) Unentangled network with $\phi_1=\phi_2=\theta/2$. For the entangled network the amount of electron current in the $|1\rangle_A$ state is large compared to the $|0\rangle_A$ state for phase angle $\theta$ near $\pi$. The opposite is true for the unentangled network.

network is plotted in Fig. 4. We see that the amount of probability exiting the $|1\rangle$ waveguide in relation to the $|0\rangle$ waveguide of qubit $A$ is much greater for the entangled network than the unentangled network for phases angles near $\pi$. There is a significant range of phase angles when the two networks would be distinguishable.

In the situation above we have used the spatial symmetry of the network to set $\phi_1=\phi_2=\theta/2$ for a nonentangling gate $\hat{V}$. An imperfect nonentangling gate need not split the phase angle $\theta$ equally between the two individual qubits. We then write $\phi_2=\theta-\phi_1$ and, given an input state $|\Phi_L\rangle=|1,1\rangle$, we analyze the output of the network as both $\theta$ and $\phi_1$ are varied. We find that when $\theta=\pi$ the output states of the entangling network and the nonentangling network are distinguishable for all values of $\phi_1$. As above, the networks are most distinguishable when $\phi_1=\phi_2=\pi/2$. For the entangling network, the probability of finding the output state $|\Phi_R\rangle=|0,1\rangle$ when $\theta=\pi$ is 1. For the nonentangling network, the probability of finding the output state $|\Phi_R\rangle=|0,1\rangle$ when $\theta=\pi$ is never larger than 1/4 for all values of $\phi_1$.

## III. DYNAMIC MODEL OF COULOMB ENTANGLER

In Akguc *et al.* [2], we presented a static model of Coulomb coupling between electrons in separate leads of a waveguide quantum network. We considered two parallel waveguide leads belonging to separate qubits, corresponding, for example, to the $|1\rangle$ states in the two qubits. We introduced a dielectric window between the leads that allowed electrons in the two leads to interact via their Coulomb interaction if they pass the dielectric window at the same time. We assumed that each electron produces a repulsive potential barrier in the path of the electron in the opposite lead. We then found that for certain energies the electrons could resonantly pass the barrier and create a phase shift of $e^{i\pi/2}$ for each electron state, giving an overall phase shift of $e^{i\pi}$ for the network state $|1,1\rangle$. In this and the next sections, we reexamine that picture but with a dynamic model of the actual scattering process.

In order to obtain an exactly soluble model of the scattering process, we simplify the model slightly. In the waveguide network, the actual scattering process takes place in the fixed (in space) dielectric window if two electrons (in different waveguides) pass that window at the same time. The interaction they feel will be that of a finite-range repulsive pulse (due to their mutual Coulomb interaction) whose shape, width, and strength are determined by the shape and width of the dielectric window and the distance between the waveguide leads. In our dynamic model we will neglect the dependence on the repulsive interaction due to the finite transverse width of the waveguide leads and we will allow the electrons to interact when they come within the range of their mutual repulsive interaction. We will choose our initial conditions so that this interaction occurs in a certain interval of space. Below we first consider a classical version of the model, and then we consider the fully quantum scattering process.

### A. Classical model of Coulomb entangler

Let us consider two one-dimensional straight wires, infinitely long in the $x$ direction and separated by a distance $d$ in the $y$ direction. Electron $A$ travels in the upper wire, and electron $B$ travels in the lower wire. Both electrons travel in the positive $x$ direction in their respective wires. We assume that the two electrons have nearly the same kinetic energy. Their velocities differ only by a small amount so that $v_A=v_0+\Delta v$ and $v_B=v_0-\Delta v$. Initially the separation of the two particles in the $x$ direction is large enough that no appreciable interaction takes place. We assume that electron $A$ is initially to the left of electron $B$ but is closing the gap between them as they move up the $x$ axis.

We can write the total Hamiltonian for the system in the form

$$H=\frac{1}{2m}{p_A}^2+\frac{1}{2m}{p_B}^2+\frac{V_0}{\cosh^2[\alpha(x_A-x_B)]}=E_{tot}, \qquad (6)$$

where $p_A=mv_A$ and $x_A$ ($p_B=mv_B$ and $x_B$) are the momentum and position of particle $A$ (particle $B$), $V_0$ is the maximum interaction strength, $1/\alpha$ is the width of the interaction potential between the two electrons, and $E_{tot}$ is the total energy of the system. In a Coulomb-like interaction the distance between the wires, $d$, determines the maximum interaction strength $V_0$ between the particles but otherwise does not add to an understanding of the interaction itself.

The center-of-mass momentum and position of the electrons are $P=p_A+p_B$ and $X=\frac{1}{2}(x_A+x_B)$, respectively. Their relative momentum and position are $x=x_A-x_B$ and $p=\frac{1}{2}(p_A-p_B)$, respectively. In terms of these coordinates, the Hamiltonian takes the form

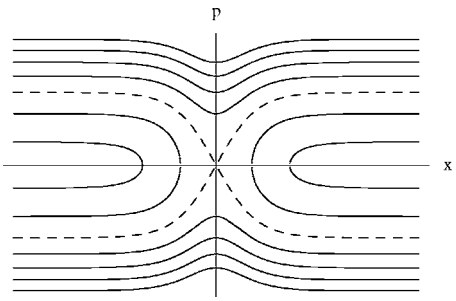


FIG. 5. The phase space of the relative motion. The dashed line is the separatrix between electrons with relative energy $0<E_r<V_0$ and electrons with relative energy $V_0<E_r<\infty$. Electrons with relative energy $0<E_r<V_0$ (inside the separatrix) interchange their momenta during the collision and not their relative postions. Trajectories with relative energy $V_0<E_r<\infty$ (outside the separatrix) interchange their position and not their momenta during the collision. (All units dimensionless.)

$$H=\frac{P^2}{4m}+\frac{p^2}{m}+\frac{V_0}{\cosh^2(\alpha x)}=E_{tot}. \tag{7}$$

We see that the center-of-mass momentum and the center-of-mass energy $E_{\text{c.m.}}=P^2/4m$ are constants of the motion.

All the interesting dynamics occurs in the relative motion of the two electrons whose Hamiltonian is given by

$$H_r=\frac{p^2}{m}+\frac{V_0}{\cosh^2(\alpha x)}=E_r, \tag{8}$$

where $E_r$ is the energy contained in the relative motion of the particles. The character of this motion is determined by the relationship between the energy of relative motion, $E_r=E_{tot}-E_{\text{c.m.}}$, and the interaction strength $V_0$. The phase-space diagram for the relative motion is plotted in Fig. 5. Electrons with relative energy $0<E_r<V_0$ interchange their momenta during the collision but not their relative postions (the phase-space motion corresponds to the curves that cross the $x$ axis in Fig. 5). Trajectories with relative energy $V_0<E_r<\infty$ interchange their position and not their relative momenta during the collision (the curves that cross the $p$ axis in Fig. 5).

The case where electrons $A$ and $B$ have approximately the same velocity—so $v_A=v_0+\Delta v$ and $v_B=v_0-\Delta v$ with $\Delta v \ll v_0$ and both travel in the positive $x$ direction—corresponds to the case $0<E_r<V_0$. Electron $A$ will catch up to electron $B$ and they will undergo a collision with the result that they interchange their velocities but not their positions. We combine the solutions for the center-of-mass coordinate and the relative coordinate for the case $E_r<V_0$ and obtain

$$x_A(t)=\sqrt{\frac{E_{\text{c.m.}}}{m}}t-\frac{1}{2\alpha}\sinh^{-1}\left[\sqrt{\frac{V_0}{E_r}-1}\times\cosh\left(-\alpha\sqrt{\frac{4E_r}{m}}t\right)\right]. \tag{9}$$

and

$$x_B(t)=\sqrt{\frac{E_{\text{c.m.}}}{m}}t+\frac{1}{2\alpha}\sinh^{-1}\left[\sqrt{\frac{V_0}{E_r}-1}\times\cosh\left(+\alpha\sqrt{\frac{4E_r}{m}}t\right)\right]. \tag{10}$$

For these solutions, the interaction is centered at $x=0$ at time $t=0$. In the asymptotic regions where both particles are far away from the interaction ($t\to\infty$, $t\to-\infty$) the particles move with constant velocity. The particles exchange velocity during the interaction and do not pass each other.

In ballistic electron waveguides built using GaAs—$Al_xGa_{1-x}As$ heterostructures the energy of the traveling electrons at low temperatures is very close to the Fermi energy of the electron gas [6]. We would therefore expect that the energies of any two electrons traveling through a Coulomb coupler structure would be quite similar, resulting in a small relative energy with respect to the interaction potential. This corresponds classically to the case $E_r<V_0$ considered above.

### B. Quantum scattering model of Coulomb entangler

Let us now consider the quantum realization of the classical model described above. The Schrödinger equation for the two-particle system is

$$-\frac{\hbar^2}{2m}\left(\frac{\partial^2}{\partial x_A^2}+\frac{\partial^2}{\partial x_B^2}\right)\Psi+\frac{V_0\Psi}{\cosh^2[\alpha(x_A-x_B)]}=E_{tot}\Psi, \tag{11}$$

where $\Psi=\Psi(x_A,x_B)$ is the energy eigenstate of the two-particle system. If we again change to center-of-mass and relative coordinates, the Schrödinger equation takes the form

$$-\frac{\hbar^2}{2m}\left(\frac{1}{2}\frac{\partial^2}{\partial X^2}+2\frac{\partial^2}{\partial x^2}\right)\Psi+\frac{V_0\Psi}{\cosh^2(\alpha x)}=E\Psi, \tag{12}$$

where $\Psi$ is now a function of the center-of-mass and relative coordinates. The center-of-mass momentum and energy are again constants of motion for this system. We assume a separable form for the two-particle wave function, $\Psi(X,x)=\psi(X)\phi(x)$. The solution for the center-of-mass wave function is

$$\psi(X)=e^{iKX}, \tag{13}$$

where $K=P/\hbar=\sqrt{4mE_{\text{c.m.}}/\hbar^2}$ is the center-of-mass wave vector. The solution for the wave function describing the relative motion is [7]

$$\phi(x)=(1-\zeta^2)^{-ik/2\alpha}F\left(\frac{-ik}{\alpha}-s,\frac{-ik}{\alpha}+s+1,\frac{-ik}{\alpha}+1,\frac{1}{2}(1-\zeta)\right), \tag{14}$$

where $F$ is a hypergeometric function, $k=\sqrt{mE_r/\hbar^2}$, $\zeta=\tanh(\alpha x)$, and $s=\frac{1}{2}(-1+\sqrt{1-4mV_0/\alpha^2\hbar^2})$. The center-of-mass solution $\psi(X)$ is chosen to represent the state of two particles traveling in the positive $x$ direction and is normalized to unity.

We are considering the scattering of two electrons for the case $E_r<V_0$, traveling along the pair of waveguides in the

positive $x$ direction. Initially the electrons enter the system from the left such that electron $A$ begins to the left of electron $B$ and electron $A$ has a slightly larger momentum than electron $B$. The repulsive interaction potential between the two electrons falls off rapidly enough that asymptotically ($t \rightarrow \pm\infty$) the electrons are free.

From the discussion of the classical version of this problem (for $E_r < V_0$) we see that there are two asymptotic regimes. In one regime ($x \rightarrow -\infty$), electron $A$ remains to the left of electron $B$, but during the collision they interchange momenta (this is the only case that is allowed classically). However, quantum mechanically the regime ($x \rightarrow +\infty$) is also allowed. This would require the wave function to tunnel through the barrier in the relative motion problem. We can now write the asymptotic form of the solution for the relative motion problem in the form

$$\phi(x \rightarrow \infty) = Te^{ikx}, \quad \phi(x \rightarrow -\infty) = e^{ikx} + Re^{-ikx}. \quad (15)$$

The coefficient $T$ is the probability amplitude that the electrons interchange position and not momentum during the collision. The coefficient $R$ is the probability amplitude that the electrons interchange momentum and not postion during the collision (the classically allowed case). The term $e^{ikx}$ is the wave function for the relative motion before the collision. If we take the asymptotic limits ($x \rightarrow \pm\infty$) of the hypergeometric function, we obtain the following expressions for the probability amplitudes $T$ and $R$:

$$T = \frac{\Gamma\left(\frac{-ik}{\alpha} - s\right)\Gamma\left(\frac{-ik}{\alpha} + s + 1\right)}{\Gamma\left(\frac{-ik}{\alpha}\right)\Gamma\left(\frac{-ik}{\alpha} + 1\right)}, \quad (16)$$

$$R = \frac{\Gamma\left(\frac{ik}{\alpha}\right)\Gamma\left(\frac{ik}{\alpha} - s\right)\Gamma\left(\frac{ik}{\alpha} + s + 1\right)}{\Gamma\left(\frac{-ik}{\alpha}\right)\Gamma(-s)\Gamma(s+1)}, \quad (17)$$

where $\Gamma(x)$ is the gamma function.

We can now write the total wave function for the system in the asymptotic regions ($x_A \rightarrow -\infty$, $x_B \rightarrow -\infty$) and ($x_A \rightarrow +\infty$, $x_B \rightarrow +\infty$). For ($x_A \rightarrow -\infty$, $x_B \rightarrow -\infty$) the total wave function is

$$\Psi(x_A, x_B) = e^{ik_A x_A} e^{ik_B x_B}, \quad (18)$$

where $k_A = p_A/\hbar$ and $k_B = p_B/\hbar$ are the incident wave vectors of electrons $A$ and $B$. For ($x_A \rightarrow +\infty$, $x_B \rightarrow +\infty$) the total wave function is

$$\Psi(x_A, x_B) = Te^{ik_A x_A} e^{ik_B x_B} + Re^{ik_B x_A} e^{ik_A x_B}. \quad (19)$$

This simple model of Coulomb entanglement predicts no reflection of an individual electron due to the collision, but simply a mutual phase shift of the two electrons and a possible exchange of momenta. This bodes well for future implementations of such structures in quantum processing devices, as reflection of individual electron probability at the computational gates plays a large role in determining the fidelity of a computation [2,3].

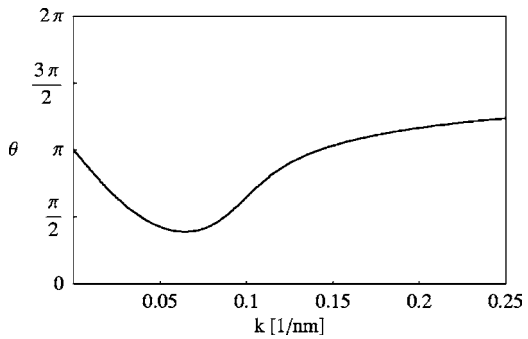


FIG. 6. Plot of the phase angle $\theta$ of the probability amplitude $R = e^{i\theta}$ versus relative momentum $k$. The phase angle is very near $\pi$ when the relative momentum is very small.

As stated above, in ballistic electron waveguides in GaAs—$Al_xGa_{1-x}As$ semiconductor heterostructures the incoming energies of each electron is expected to be near the Fermi energy of the device, $E_F$. We assume that widths of the waveguides are equal so that the energy required for the first transverse mode is the same. For electrons in the first propagating channel of the waveguide leads, this means that the momenta of the electrons will be given by $k_A = \sqrt{2m(E_F \pm \delta_E)/\hbar^2 - (\pi/w)^2}$ and $k_B = \sqrt{2m(E_F \pm \delta_E)/\hbar^2 - (\pi/w)^2}$ where $\delta_E$ is the deviation in energy from the Fermi energy due to the finite temperature of the semiconductor material. For low temperatures we can expect $\delta_E$ to be very small and therefore the relative momentum of the two electrons to be very small. From the above discussion, we see that as the relative momentum $k \rightarrow 0$, $R \rightarrow -1$, and $T \rightarrow 0$. This would correspond to the electrons exchanging momentum and leaving the interaction region with a mutual phase change of $e^{i\pi}$. This is just what is needed to obtain optimum entanglement in the network described in the previous section.

To determine how the reflection and transmission amplitudes might vary in an implementation of the network at finite temperature, we use numerical values similar to those used in [2] for GaAs—$Al_xGa_{1-x}As$ quantum networks. We define a unit of length, $\omega_0 = 40$ nm, and a unit of energy, $E_0 = \hbar^2/2m\omega_0^2 = 0.000\,355$ eV, where $m = 0.067m_e$ is the effective electron mass in GaAs—$Al_xGa_{1-x}As$ semiconductor structures and $m_e$ is the mass of the free electron. If we assume that the leads have a transverse width $w = 160$ Å, the electrons propagate in the first channel for Fermi energies $61.7 \leqslant E_F/E_0 \leqslant 246.8$. We use an interaction potential of $V_0 = 32.14E_0$ and an interaction region of length $1/\alpha = \omega_0/2$. Figure 6 shows the behavior of the phase angle of the reflection amplitude as the relative momentum varies. For small values of the relative momentum the reflection amplitude and, therefore, the mutual phase between the electron currents approach $e^{i\pi}$. Figure 7 shows how the reflection probability varies with the relative momentum. Reflection dominates for small relative momentum.

In order to maintain quantum coherence in these types of devices, temperatures must be on the order of a few kelvins [6]. When both qubits are formed at the same semiconductor heterostructure we can assume the same Fermi energy value in both qubit structures. At the low temperatures associated

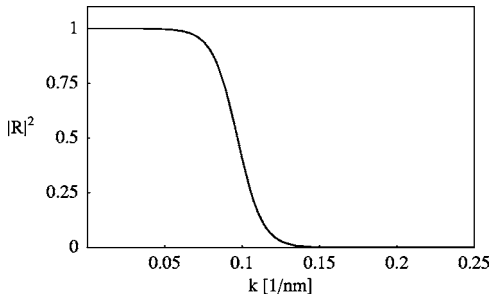


FIG. 7. The probability $|R|^2$ of momentum exchange during the collision.

with these types of semiconductor devices the electrons travel with an energy very near the Fermi level. Therefore the average deviation from the Fermi level of each of our two traveling electrons corresponds to the relative energy of the electrons incident on the interaction region. At small temperatures the electron energy deviates from the Fermi energy an average amount $\delta_E \approx k_B T$, where $k_B$ is Boltzmann's constant and $T$ is the temperature. For a temperature of 4 K we find the average separation in energy to be $\delta_E \approx E_0$. This allows us to find the average deviation in each electron longitudinal momentum $\delta_k$. Taking values for the leads of width $w=160$ Å and Fermi energy $E_F/E_0=150$ we find $\delta_k \approx 0.0027$ nm$^{-1}$. Then using a relative momentum of $k=\delta_k$ we find near unit probability for momentum exchange and an amplitude phase angle very near $\pi$ so that the phase angle of the amplitude, $R=e^{i\theta}$, is $\theta=\pi\pm\delta_\theta$ where $\delta_\theta=0.13$ rad.

## IV. CONCLUSIONS

We have presented a network for the testing of entanglement in ballistic electron waveguide qubits. The entangling properties of the Coulomb gate are distinguishable for phase angles close to $\pi$. The simple model of a Coulomb-like coupler predicts a mutual phase angle of the $|1, 1\rangle$ state very near $\pi$ when the relative momentum between the two particles is very small. There is no reflection of individual electrons at the Coulomb region. All incoming probability continues forward through the Coulomb coupler region towards the output side of the network.

## ACKNOWLEDGMENTS

The authors thank the Robert A. Welch Foundation (Grant No. F-1051) and the Engineering Research Program of the Office of Basic Energy Sciences at the U.S. Department of Energy (Grant No. DE-FG03-94ER14465) for support of this work. L.E.R. thanks the Office of Naval Research (Grant No. N00014-03-1-0639) for partial support of this work.

[1] Radu Ioniciouiu, Gehan Amaratunga, and Florin Udrea, Int. J. Mod. Phys. B **15**, 125 (2001).
[2] Gursoy B. Akguc, Linda E. Reichl, Anil Shaji, and Michael G. Snyder, Phys. Rev. A **69**, 042303 (2004).
[3] Michael G. Snyder and Linda E. Reichl, Phys. Rev. A **70**, 052330 (2004).
[4] S. Datta, *Electronic Transport in Mesoscopic Systems* (Cambridge University Press, Cambridge, England, 1995).
[5] J. Harris, R. Akis, and D. K. Ferry, Appl. Phys. Lett. **79**, 2214 (2001).
[6] J. P. Bird, R. Akis, D. K. Ferry, A. P. S. de Moura, Y.-C. Lai, and K. M. Indlekofer, Rep. Prog. Phys. **66**, 583 (2003).
[7] L. D. Landau and E. M. Lifshitz, *Quantum Mechanics* (Pergamon, New York, 1977).